*Journal of Zhejiang University-SCIENCE B (Biomedicine & Biotechnology) 2024 25(8):686-699*
www.jzus.zju.edu.cn; www.springer.com/journal/11585
E-mail: jzus_b@zju.edu.cn

**Research Article**
https://doi.org/10.1631/jzus.B2300407



# Single-cell transcriptomics reveals tumor landscape in ovarian carcinosarcoma

Junfen XU[1,2]✉, Mengyan TU[1]

[1]*Department of Gynecologic Oncology, Women's Hospital, Zhejiang University School of Medicine, Hangzhou 310006, China*
[2]*Zhejiang Provincial Clinical Research Center for Obstetrics and Gynecology, Hangzhou 310006, China*

**Abstract:** Objective: The present study used single-cell RNA sequencing (scRNA-seq) to characterize the cellular composition of ovarian carcinosarcoma (OCS) and identify its molecular characteristics. Methods: scRNA-seq was performed in resected primary OCS for an in-depth analysis of tumor cells and the tumor microenvironment. Immunohistochemistry staining was used for validation. The scRNA-seq data of OCS were compared with those of high-grade serous ovarian carcinoma (HGSOC) tumors and other OCS tumors. Results: Both malignant epithelial and malignant mesenchymal cells were observed in the OCS patient of this study. We identified four epithelial cell subclusters with different biological roles. Among them, epithelial subcluster 4 presented high levels of breast cancer type 1 susceptibility protein homolog (*BRCA1*) and DNA topoisomerase 2-α (*TOP2A*) expression and was related to drug resistance and cell cycle. We analyzed the interaction between epithelial and mesenchymal cells and found that fibroblast growth factor (FGF) and pleiotrophin (PTN) signalings were the main pathways contributing to communication between these cells. Moreover, we compared the malignant epithelial and mesenchymal cells of this OCS tumor with our previous published HGSOC scRNA-seq data and OCS data. All the epithelial subclusters in the OCS tumor could be found in the HGSOC samples. Notably, the mesenchymal subcluster C14 exhibited specific expression patterns in the OCS tumor, characterized by elevated expression of cytochrome P450 family 24 subfamily A member 1 (*CYP24A1*), collagen type XXIII α1 chain (*COL23A1*), cholecystokinin (*CCK*), bone morphogenetic protein 7 (*BMP7*), *PTN*, Wnt inhibitory factor 1 (*WIF1*), and insulin-like growth factor 2 (*IGF2*). Moreover, this subcluster showed distinct characteristics when compared with both another previously published OCS tumor and normal ovarian tissue. Conclusions: This study provides the single-cell transcriptomics signature of human OCS, which constitutes a new resource for elucidating OCS diversity.

**Key words:** Ovarian carcinosarcoma; Single-cell RNA sequencing (scRNA-seq); Tumor heterogeneity

## 1 Introduction

Ovarian cancer is the fifth most common cause of cancer-related deaths in women. According to a report by the American Cancer Society, approximately 21 750 women were newly diagnosed with ovarian cancer in 2020, with 13 940 cases of mortality (Siegel et al., 2020). Of all reported cases of ovarian cancer, 90% are of the epithelial cell type (Kurman and Shih, 2011; Gao et al., 2022), and the remaining 10% consist of non-epithelial ovarian cancers (non-EOCs), primarily germ cell tumors, sex cord-stromal tumors, and a subset of exceptionally uncommon malignancies like small cell carcinomas (Cheung et al., 2022). Ovarian carcinosarcoma (OCS), also known as malignant mixed Müllerian tumor, is one of rarest and most challenging histological subtypes, accounting for 1%–4% of all ovarian cancer cases (del Carmen et al., 2012). Given the rarity of OCS, there is a paucity of prospective clinical trials to guide treatment strategies. Thus, the management of OCS has been mainly extrapolated from the treatment experience of EOC. However, some observational studies have reported that OCS has a distinct natural history from EOC (Rauh-Hain et al., 2011; del Carmen et al., 2012). When compared with EOC patients, the majority of OCS patients have a worse survival rate: the reported 5-year overall survival (OS) rate was shown to be 29.8%, with the median OS time ranging from 8–26 months (George et al., 2013; Rauh-Hain et al., 2013). Another study also showed

✉ Junfen XU, xjfzu@zju.edu.cn
Junfen XU, https://orcid.org/0000-0002-2377-0775

Received June 12, 2023; Revision accepted Sept. 21, 2023;
Crosschecked July 31, 2024

the poor OS of OCS with a median of 12.7 months (Hollis et al., 2022). The main epithelial components were of high-grade serous type. Heterologous elements were common such as chondrosarcoma, rhabdomyosarcoma, and liposarcoma (Hollis et al., 2022). Therefore, understanding the precise molecular alterations that occur during the progression of this malignancy remains a priority, in order to fully characterize this disease and provide evidence-based diagnostic and therapeutic treatments that will ultimately lead to improvements in the survival rate.

According to the current knowledge of OCS, this tumor type exhibits a high degree of heterogeneity and contains both malignant epithelial and sarcomatous elements (Boussios et al., 2019; Gotoh et al., 2019). OCS has been reported to be associated with overexpression of the protein 53 (*p53*) gene, and mutations were shown to be harbored in this gene (Liu et al., 1994). *Ki-67* appears to serve a critical role in OCS. Indeed, the high Ki-67 level was identified in half of OCS samples and associated with shorter survival time (Ariyoshi et al., 2000). An analysis of the Surveillance, Epidemiology, and End Results (SEER) data suggested that patients with OCS at tumor stage II and above had poor OS rates, with a hazard ratio (HR) for death in the range of 1.19–5.88. Moreover, the positive immunohistochemistry (IHC) staining of tumoral cluster of differentiation 8-positive ($CD8^+$) T lymphocytes and the negative expression of mesenchymal programmed death ligand-1 (PD-L1) were found to be associated with improved survival rates in patients with OCS (Zhu et al., 2017). Increased expression levels of vascular endothelial growth factor (VEGF) and VEGF receptor-3 (VEGFR3) and increased vessel number were associated with poor survival (Näyhä and Stenbäck, 2008). These data suggest that the tumor microenvironment (TME) may play important roles in governing the plasticity of the phenotypic traits of tumor cells as well as in mediating the response to therapies. Unfortunately, conventional bulk sequencing techniques have limitations in terms of their ability to map the TME. On the other hand, recent advances in single-cell RNA sequencing (scRNA-seq) have given novel insights into tumor composition and characterization of the molecular properties of complex tissues at a cellular level of resolution (Ding et al., 2020; Lee et al., 2020; Luo et al., 2020; Ma et al., 2020; Maynard et al., 2020). This technique provides unique opportunities to explore the complexity of TME, revealing detailed information about the regulation and evolution of or interaction among individual cells. However, to date, studies of OCS have lacked a higher-resolution formation on cellular heterogeneity, prompting the need for an improved understanding of tumor cells and the distribution of stromal and immune cells in the TME for more successful putative clinical strategies to treat OCS.

In the present study, scRNA-seq was applied to resected primary OCS for an in-depth analysis of the tumor cells and their TME. The results uncovered the characteristics of various cell populations of OCS and are expected to provide important clues for the development of OCS therapeutic strategies.

## 2 Results

### 2.1 Single-cell transcriptional atlas analysis and cell composition in OCS tissues

One primary ovarian sample obtained from a patient with OCS was characterized using scRNA-seq on the 10x Genomics Chromium platform (https://www.10xgenomics.com). The 61-year-old female patient was diagnosed with OCS at a late tumor stage (stage IIIC) with omental metastases. The computed tomography (CT) and magnetic resonance imaging (MRI) examinations of this case indicated that the main feature was a massive ovarian tumor (Fig. 1a) and no obvious tumor was observed within the uterus. The pathological results further confirmed a normal endometrium, with the tumor only affecting the surface of the uterus. Hematoxylin and eosin (H&E) staining and IHC staining were conducted to establish the diagnosis of OCS (Figs. 1b and S1). IHC staining for cytokeratin (CK) and E-cadherin revealed diffuse strong staining of the epithelial component (Fig. S1). The mesenchymal element was stained for vimentin and desmin (Fig. S1). The tumor presented with high levels of the cellular proliferation markers Ki-67 and p16, as shown by the labeling indexes (Fig. S1). In addition, overexpression of the mutant *p53* was found in the OCS tumor, suggesting a high-grade serous epithelial type (Fig. S1). Previous studies have demonstrated that *Ki-67* and *p53* overexpression affects OS rate of the OCS (Ariyoshi et al., 2000; Zorzou et al., 2005). We also showed that this patient expressed focal programmed death-1 (PD1) (Fig. S1). A recent study reported that

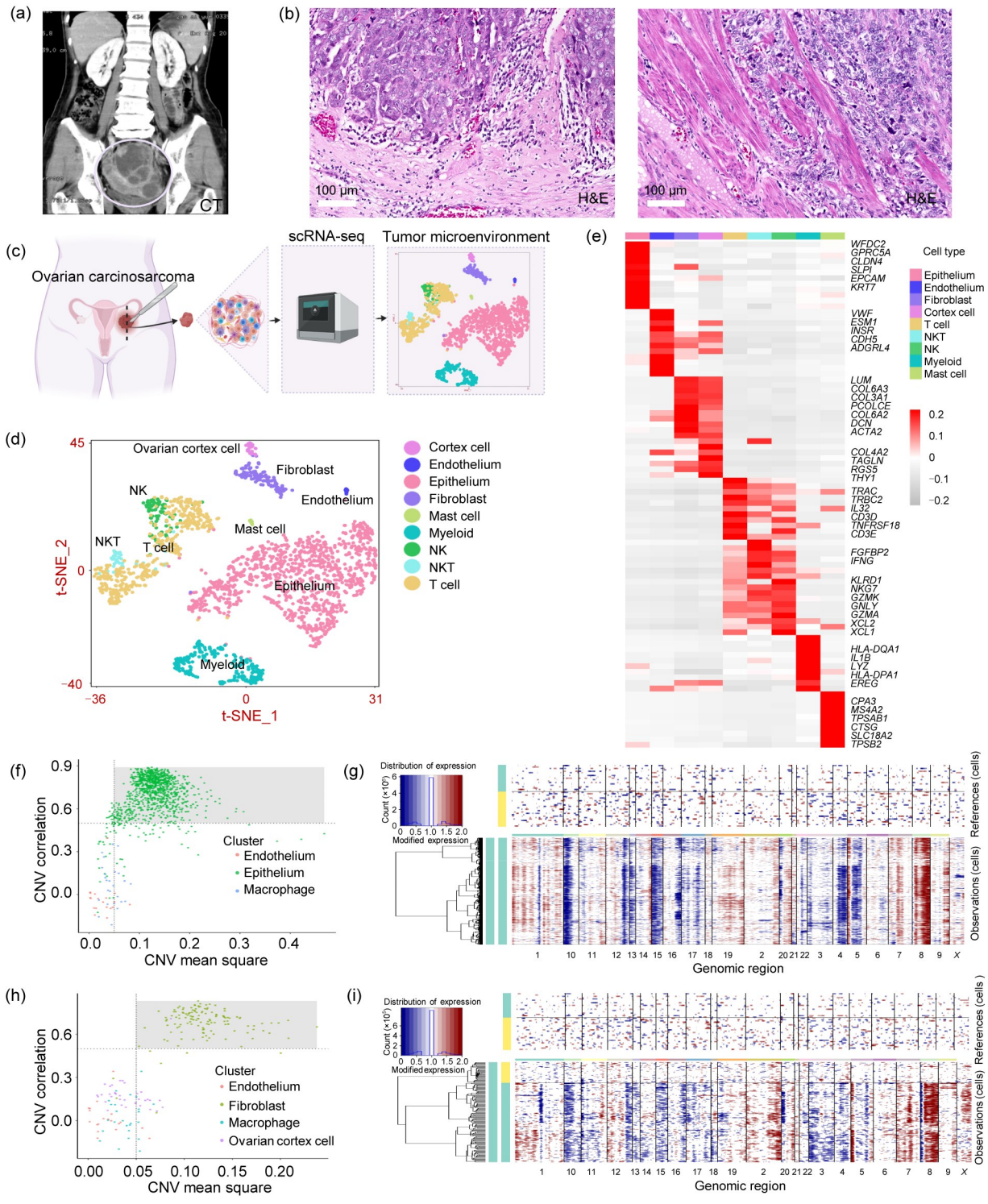


**Fig. 1 Identification of ovarian carcinosarcoma (OCS) cell populations. (a) Computed tomography (CT) scan showing the location and volume of OCS. (b) Hematoxylin and eosin (H&E) staining in OCS tissue. (c) Schematic diagram of single-cell RNA sequencing (scRNA-seq) analysis workflow. (d) The t-distributed stochastic neighbor embedding (t-SNE) plots for the cell type identification of 2173 high-quality single cells in OCS. (e) Heatmap showing the expression levels of specific markers in each cell type. (f, h) Copy number variation (CNV) score and correlation for each indicated cell. Grey: CNV score is >0.05 and CNV correlation is >0.5. (g, i) Inferred large-scale CNVs help identify malignant and non-malignant cells. Amplifications (red) or deletions (blue) were inferred by averaging expression over 100-gene stretches on the respective chromosomes. NK: natural killer; NKT: natural killer T.**

pembrolizumab was able to provide tumor control in a patient with metastatic OCS (Zibetti Dal Molin et al., 2018).

In order to further explore the features of the complex cellular components of OCS, a customized workflow to isolate viable single cells from the primary surgical resections was followed (Fig. 1c). Among the cells sequenced, 2173 were retained after quality control filtering. According to a graph-based clustering method (see supplementary "Materials and methods"), cell clusters were annotated as epithelial cells, fibroblasts, ovarian cortex cells, endothelial cells, T cells, natural killer (NK) cells, natural killer T (NKT) cells, or myeloid cells (Fig. 1d) according to established marker genes (Fig. 1e). All cell clusters identified from the OCS tumor could be visualized by combined t-distributed stochastic neighbor embedding (t-SNE) plots (Fig. 1f). For example, endothelial cells were characterized by the upregulation of von Willebrand factor (*VWF*), cadherin 5 (*CDH5*), and adhesion G protein-coupled receptor L4 (*ADGRL4*) genes, and epithelial cells were enriched with the genes epithelial cell adhesion molecule (*EPCAM*), keratin 7 (*KRT7*), and G protein-couple receptor class C group 5 member A (*GPRC5A*). Of note, the epithelial cancer cells were the main cell type of this OCS sample, comprising 52% of the sorted cells. The fibroblasts expressed high levels of decorin (*DCN*), collagen type III α1 chain (*COL3A1*), and lumican (*LUM*), whereas the mast cells featured high expression levels of carboxypeptidase A3 (*CPA3*), tryptase β2 (*TPSB2*), and cathepsin G (*CTSG*). Myeloid cells were characterized by the overexpression of major histocompatibility complex class II DQ α1 (*HLA-DQA1*), lysozyme (*LYZ*), and interleukin 1β (*IL1B*); NK cells were enriched with granulysin (*GNLY*), natural killer cell granule protein 7 (*NKG7*), and killer cell lectin like receptor D1 (*KLRD1*); NKT cells exhibited high expression levels of fibroblast growth factor-binding protein 2 (*FGFBP2*); and T cells were characterized by the overexpression of T cell receptor α constant (*TRAC*) and the CD3 epsilon subunit of T-cell receptor complex (*CD3E*). Finally, the ovarian cortex cells were enriched by transgelin (*TAGLN*), *RSG5*, and Thy-1 cell surface antigen (*THY1*) (Fig. S2).

### 2.2 Malignant elements from non-cancer cells resolved by clustering-based copy number variation

Cancer cells are known to be associated with large-scale chromosomal alterations (Thompson and Compton, 2011; Maynard et al., 2020). In the present study, copy number variation (CNV) from the RNA expression data was applied to classify epithelial cells as either cancerous or non-cancerous by comparison with endothelial cells and macrophages (controls). As shown in Figs. 1f and 1g, the epithelial cancer cells displayed much larger variations from the relative expression intensities across the genome. Notably, OCS contains both malignant epithelial and sarcomatous (mesenchymal) elements (del Carmen et al., 2012). Therefore, we utilized CNV to verify whether fibroblasts and ovarian cortex cells were the malignant sarcomatous elements. As shown in Figs. 1h and 1i, fibroblasts were found to display much larger chromosomal changes across the genome relative to endothelial cells and macrophages but not the ovarian cortex cells. Fig. S3 further displays the t-SNE plot distribution of malignant epithelial and malignant mesenchymal cells in the total cell population based on the CNV results. The expression levels of the epithelial cell markers EPCAM and KRT7 and the fibroblast markers DCN and COL3A1 (Fig. S1) were further validated in human OCS tumor tissues by IHC staining (Fig. S2). Taken together, the results of the malignant cell clustering analysis corroborated that epithelial cells and mesenchymal cells were the two malignant sources of OCS.

### 2.3 Transcriptional landscape intra-tumoral heterogeneity of OCS epithelial cells

Subsequently, detailed clustering analysis of the epithelial cells was performed using Seurat, which revealed the existence of four prominent cell subpopulations, namely, C1 (calgranulin-B (*S100A9*)$^+$/carcinoembryonic antigen-related cell adhesion molecule 6 (*CEACAM6*)$^+$/S100 calcium-binding protein P (*S100P*)$^+$/keratin, type II cytoskeletal 6A (*KRT6A*)$^+$), C2 (insulin-like growth factor-binding protein 3 (*IGFBP3*)$^+$/stanniocalcin-2 (*STC2*)$^+$/max-like protein 1 (*MXL1*)$^+$/adhesion G protein-coupled receptor B1 (*ADGRB1*)$^+$), C3 (cadherin-6 (*CDH6*)$^+$/regulator of G-protein signaling 16 (*RGS16*)$^+$/asparaginase-like protein 1 (*ASRGL1*)$^+$/protein wntless (*WLS*)$^+$), and C4 (centromere protein F (*CENPF*)$^+$/DNA topoisomerase 2-α (*TOP2A*)$^+$/proliferation marker protein Ki-67 (*MKI67*)$^+$) (Figs. 2a and 2b). To learn more about the biology underlying these cell subgroups, the Kyoto Encyclopedia of Genes and Genomes (KEGG) pathway analysis

was first employed to identify distinct signaling pathways, and transcription factor consensus sites were sought after using the single-cell regulatory network inference and clustering (SCENIC) method (Figs. 2c and 2d). These analyses confirmed that the C1 subpopulation was controlled by the transcription factor Hes

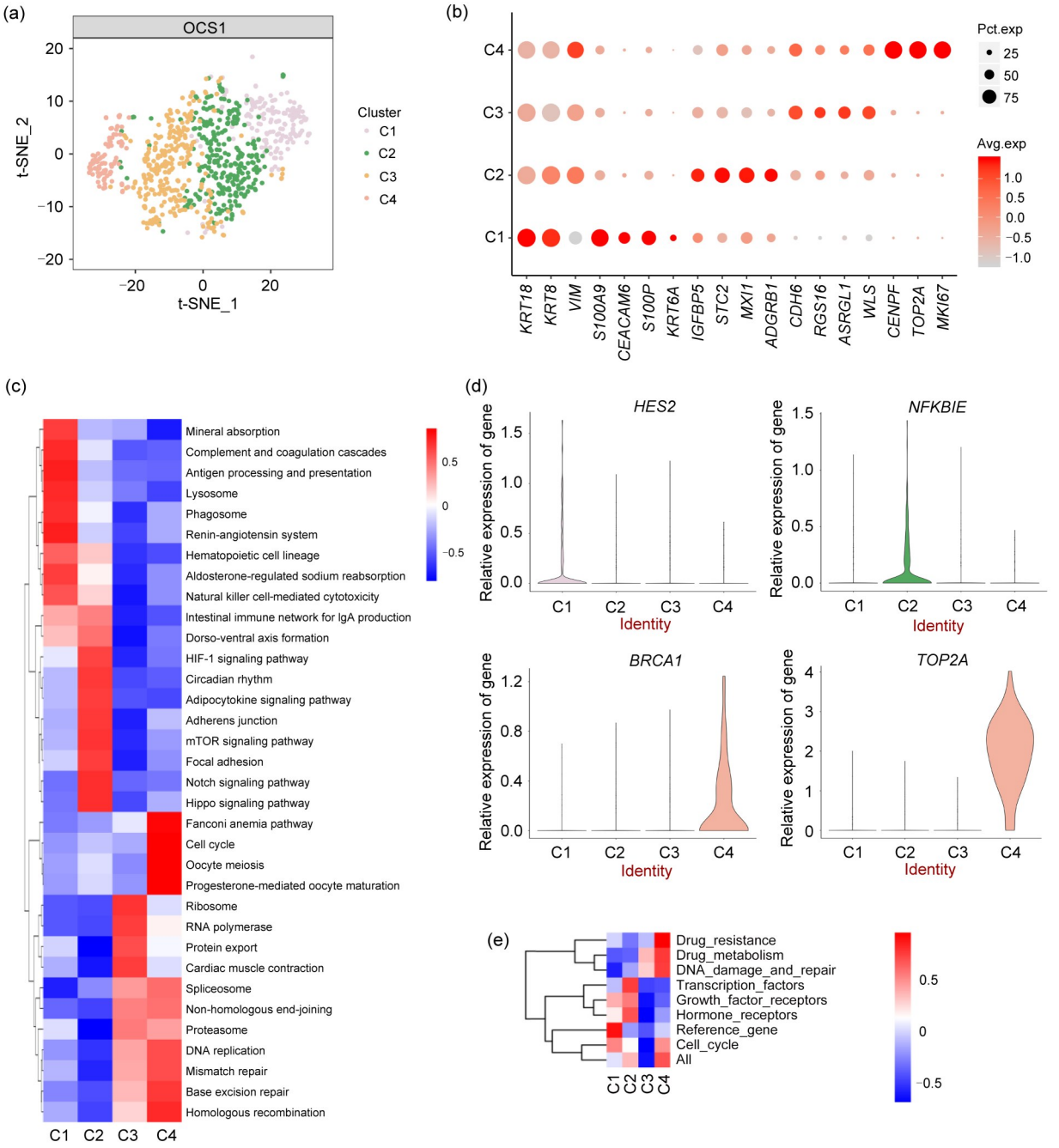


**Fig. 2 Transcriptomic heterogeneity of epithelial cells in ovarian carcinosarcoma (OCS). (a) The t-distributed stochastic neighbor embedding (t-SNE) plots for color-coded four distinct epithelial cell subclusters. (b) Gene bubble plots illustrating different marker genes in each cell subtype. (c) Differences in pathway activity in epithelial cell subclusters. (d) Violin plots illustrating the expression of specific transcription factors in distinct epithelial cell subclusters. (e) Heatmap showing the different drug resistance-related pathways in four epithelial cell subclusters. *HES2*: Hes family basic helix-loop-helix (bHLH) transcription factor 2; *NFKBIE*: nuclear factor-κB inhibitor epsilon; *BRCA1*: breast cancer type 1 susceptibility protein homolog; *TOP2A*: DNA topoisomerase 2-α; Pct.exp: percent expressed; Avg.exp: average expression; IgA: immunoglobulin A; HIF-1: hypoxia inducible factor-1; mTOR: mammalian target of rapamycin.**

family basic helix-loop-helix (bHLH) transcription factor 2 (HES2), and was enriched for the antigen processing and presentation, lysosome, and phagosome pathways. The C2 subpopulation exhibited a distinct signature of the hypoxia inducible factor-1 (HIF-1), mechanistic target of rapamycin (mTOR), Notch, and hippo signaling pathways, and expressed a high level of nuclear factor-κB inhibitor epsilon (NFKBIE). The C3 subpopulation displayed increased levels of ribosome and protein export. Finally, the C4 subpopulation was found to be controlled by an elevated level of breast cancer type 1 susceptibility protein homolog (BRCA1), as well as TOP2A, and was enriched with cell cycle, Fanconi anemia pathway, and homologous recombination. Subsequently, our focus was on drug resistance analysis; we further characterized the potential drug-resistant states of the cell subpopulations in detail. These data revealed that the C4 cells had the highest levels of drug resistance scores (Fig. 2e). Interestingly, this subcluster also harbored activated drug metabolism and was positively correlated with DNA damage and repair (Fig. 2e).

### 2.4 Distinct mesenchymal cell subpopulations in the human OCS tumor

The malignant mesenchymal cells were clustered in two subpopulations (Fig. 3a). These two subclusters expressed high levels of canonical fibroblast markers, including *DCN* and *COL3A1*; however, each subcluster displayed distinct transcriptomic signatures (Fig. 3b). The C0 mesenchymal cells accounted for the majority of the mesenchymal cell populations (61.7%) that expressed high levels of extracellular matrix (ECM) signatures, including *COL6A2*, *COL6A1*, *COL3A1*, *COL6A3*, and *COL5A2*. Interestingly, the Gene Ontology (GO) analysis of this subcluster indicated significant enrichment for ECM organization and disassembly as well as angiogenesis (Fig. 3c). C1 mesenchymal cells were characterized by signature genes such as serine peptidase inhibitor kazal type 6 (*SPINK6*), RAS-like, estrogen-regulated, growth inhibitor (RERG)-like (*RERGL*), keratocan (*KERA*), STEAP2 metalloreductase (*STEAP2*), receptor activity-modifying protein 1 (*RAMP1*), and transmembrane protein 176B (*TMEM176B*). The GO terms enriched for this subcluster were associated with translational termination, translational elongation, and signal recognition particle (SRP)-dependent cotranslational protein targeting to membrane (Fig. 3c). Notably, the C0 mesenchymal cell signature was found to be enriched with a set of metabolism-associated pathways, such as linoleic acid metabolism, drug metabolism–cytochrome P450, oxidative phosphorylation, and citrate cycle (tricarboxylic acid (TCA) cycle) (Fig. 3d). However, the majority of these metabolic pathways were suppressed in C1 mesenchymal cells. The C1 signature was associated with lysine biosynthesis (Fig. 3d). As shown in Figs. 3e and 3f, the C0 mesenchymal cells expressed high levels of both type I interferon-response genes (including interferon-induced transmembrane protein 3 (*IFITM3*), interferon α-inducible protein 6 (*IFI6*), *IFITM2*, nicotinamide phosphoribosyl transferase (*NAMPT*), adenosine deaminase RNA-specific (*ADAR*), lymphocyte antigen 6E (*LY6E*), and ISG15 ubiquitin-like modifier (*ISG15*)) and type II interferon-response genes (including signal transducer and activator of transcription 1 (*STAT1*), cyclin-dependent kinase inhibitor 1A (*CDKN1A*), human leukocyte antigen-A (*HLA-A*), *HLA-B*, *HLA-C*, and *HLA-E*). This subcluster also expressed high levels of growth factors (including placental growth factor (*PGF*), *VEGFB*, insulin-like growth factor 2 (*IGF2*), pleiotrophin (*PTN*), bone morphogenetic protein 2 (*BMP2*), *BMP7*, neuropilin 1 (*NRP1*), growth differentiation factor 11 (*GDF11*), glucose-6-phosphate isomerase (*GPI*), and *VEGFA* (Fig. 3g)), chemokines (including C-C motif chemokine ligand 2 (*CCL2*), chemokine (C-X-C motif) ligand 1 (*CXCL1*), *CCL28*, and *CXCL14*), and interleukins (including *IL11* and *IL7* (Fig. S4)). These features of the C0 mesenchymal cells suggested an enrichment of the interplay between these mesenchymal cells and OCS cells.

We next analyzed the interaction between the epithelial and mesenchymal cells (Fig. 4a) and found that the fibroblast growth factor (FGF) signaling pathway and PTN signaling pathway were the main pathways contributing to the epithelial-mesenchymal communication (Fig. 4b).

### 2.5 Comparison of scRNA-seq data between OCS and published high-grade serous ovarian cancer tumors

The management of OCS has been mainly extrapolated from the treatment experience of EOC. The TME of high-grade serous ovarian cancer (HGSOC), the most common subtype of EOC, has been well studied (Geistlinger et al., 2020; Liang et al., 2021;

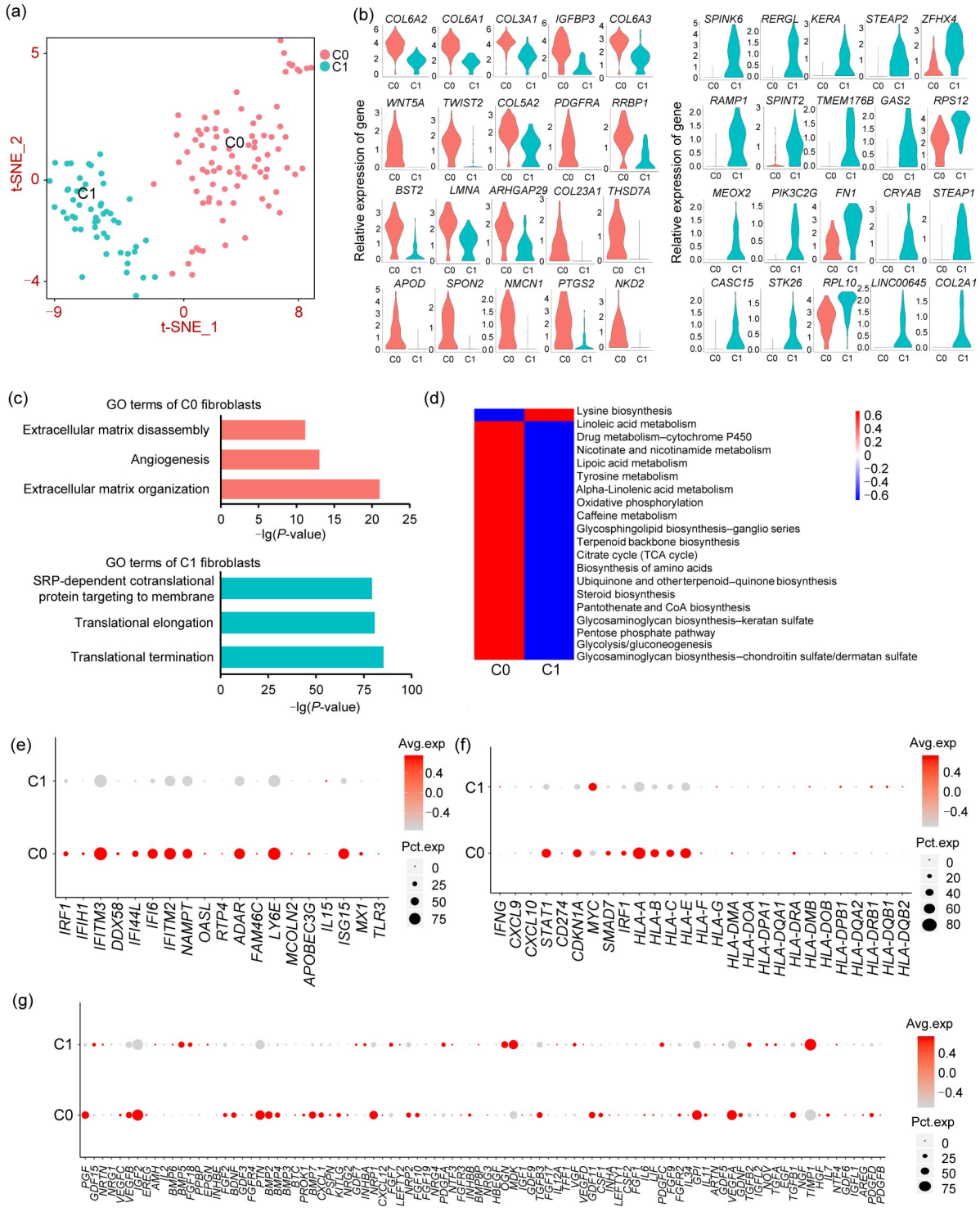


**Fig. 3 Distinct subtypes of mesenchymal cells in ovarian carcinosarcoma (OCS) tumor. (a) The t-distributed stochastic neighbor embedding (t-SNE) plots for mesenchymal cells, color-coded for two subclusters. (b) Violin plots of the expression of marker genes for each cell subtype as indicated. (c) Top 3 Gene Ontology (GO) terms for each cell subtype. (d) Heatmap indicating the differences in metabolic pathway activities in each cell subcluster. (e, f) Gene bubble plots showing different expression levels of type I (e) and type II (f) interferon (IFN)-response genes in each cell subtype. (g) Gene bubble plot illustrating the expression levels of growth factors in each cell subtype. Avg.exp: average expression; Pct.exp: percent expressed.**

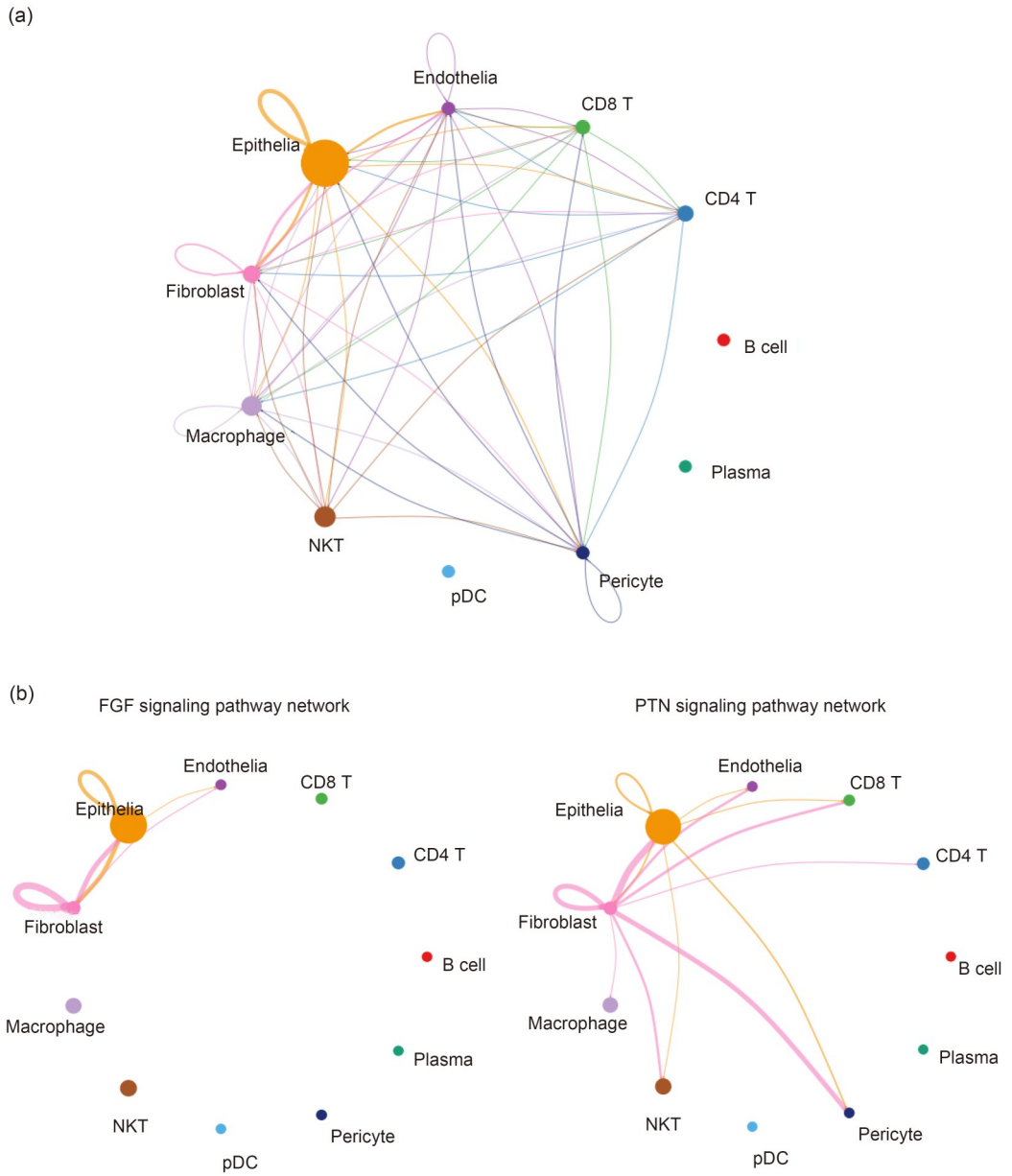


**Fig. 4 Cell–cell interactions in ovarian carcinosarcoma (OCS) as analyzed by Cell Chat program. (a) Circle plot showing the interactions and strengths among different cell types. A thicker line represents more interactions. (b) Circle plots showing the top two signaling pathways in the epithelia-mesenchymal cell communication. CD: cluster of differentiation; NKT: natural killer T; pDC: plasmacytoid dendritic cell; FGF: fibroblast growth factor; PTN: pleiotrophin.**

Liu et al., 2022; Xu et al., 2022). To determine whether there are novel subclusters in this OCS sample, we first compared the malignant epithelial cells of this OCS tumor with our previously published HGSOC scRNA-seq data (Xu et al., 2022). As shown in Figs. 5a and 5b, all the epithelial subclusters in the OCS tumor could be found in the HGSOC samples, suggesting the similarity of OCS epithelial cells to those of the HGSOC6 tumor. Moreover, the mesenchymal cell profiles were screened between the OCS tumor and our published HGSOC data (Xu et al., 2022). Our results showed that the mesenchymal cell subcluster C14 was specifically expressed in the OCS tumor with high levels of cytochrome P450 family 24 subfamily A member 1 (*CYP24A1*), collagen type XXIII α1 chain (*COL23A1*), cholecystokinin (*CCK*), *BMP7*, *PTN*, Wnt-inhibitory factor 1 (*WIF1*), and *IGF2* (Figs. 5c and 5d).

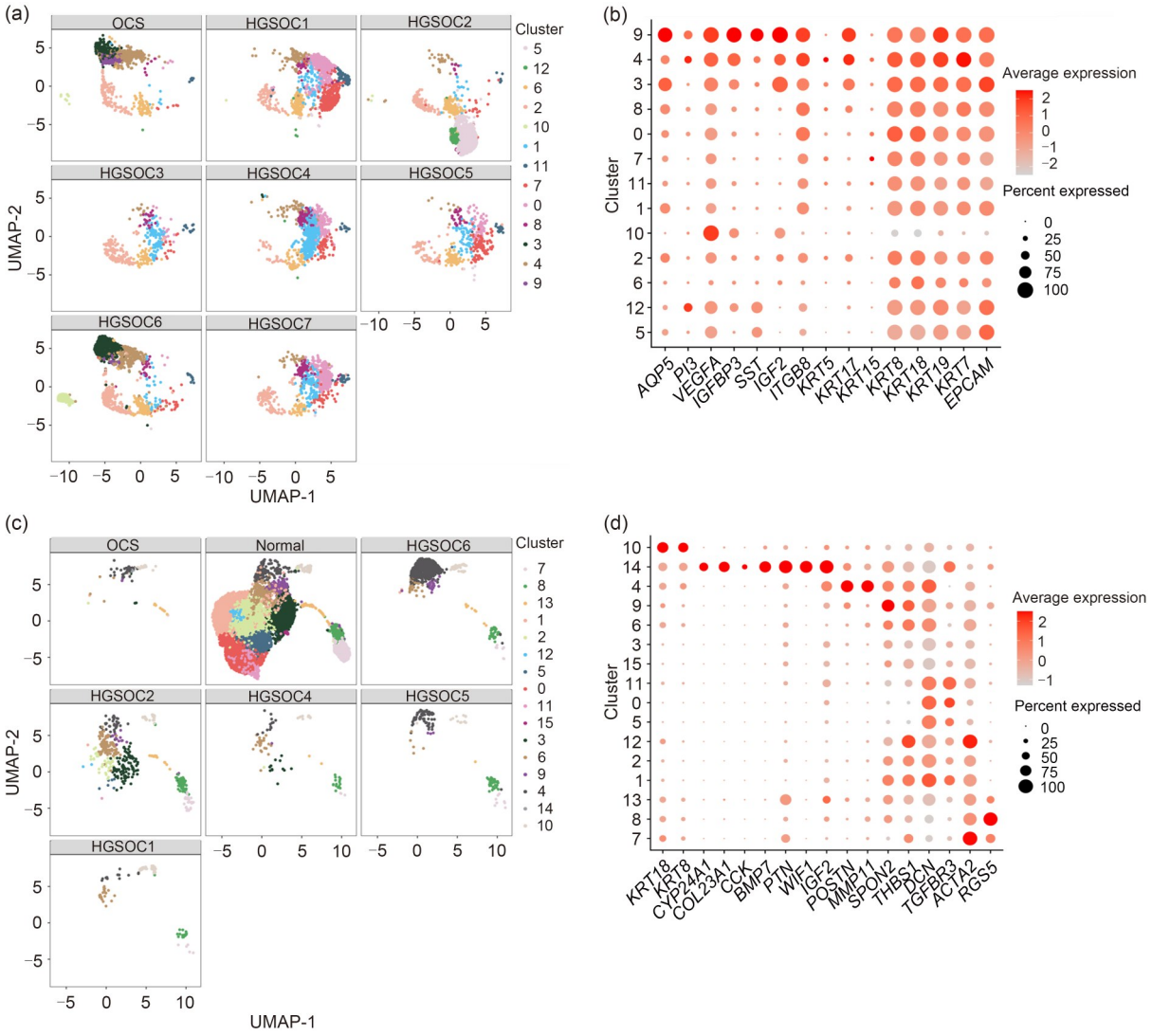


**Fig. 5 Comparison of single-cell RNA sequencing (scRNA-seq) data between ovarian carcinosarcoma (OCS) and the published high-grade serous ovarian carcinoma (HGSOC) tumors. (a) The uniform manifold approximation and projection (UMAP) plots presenting the distinct color-coded epithelial cell subclusters in this OCS tumor and the individual HGSOC tumors of our previous published study. (b) Dot plot displaying the main marker genes in each epithelial cell subcluster. (c) UMAP plots displaying the different color-coded mesenchymal cell subclusters between the OCS tumor and the individual HGSOC tumors of our previous published data. (d) Dot plot showing the main marker genes in each fibroblast subcluster.**

## 2.6 Comparison of scRNA-seq data between our OCS dataset and the previously published OCS tumor dataset as well as normal ovarian samples

As illustrated in Figs. 1d and S3, malignant mesenchymal cells constituted a minimal proportion in our OCS patient. For additional information, we searched publicly available datasets. We performed a comparative analysis between our OCS tumor scRNA-seq data and another previously published OCS tumor dataset, referred to as "3CCF1L" (Regner et al., 2021) (Figs. 6a and 6b). Notably, we observed the consistently low expression of diethylstilbestrol (DES) in both samples at the RNA level (data not shown). Subsequently, through marker analysis, we identified that troponin T1 (TNNT1) and myosin light chain 9 (MYL9), which are associated with rhabdomyosarcoma or sarcoma (Tong et al., 2014; Zhao et al., 2020), were specifically expressed in the OCS_specific_cancer-associated fibroblasts (CAFs) (referring to the mesenchymal cell subcluster C14 in Fig. 5) (Fig. 6b). This observation

suggested the presence of rhabdomyosarcoma features within this cell subpopulation. Furthermore, the OCS_specific_CAFs exhibited elevated expression levels of PTN, known for its potent growth factor secretion, and WIF1, a classic marker associated with stem cell characteristics. Collectively, these results underscored the significance of the OCS_specific_CAFs as a vital component of malignant mesenchymal cells in this OCS patient. Additionally, we conducted a comparative analysis of malignant mesenchymal cells in OCS with our previously published normal ovarian scRNA-seq data, and our findings further emphasized the heightened specificity of the OCS-specific CAF subcluster in our OCS dataset compared to normal ovaries (Figs. 6c and 6d).

For the epithelial cell comparison, the results revealed that, while there was some overlap in the epithelial cell subtypes between the two samples, in our OCS case, the cells were predominantly of the Tumor_MUC5B epithelial subtype, whereas the previously published OCS case primarily consisted of the Tumor_TAGLN epithelial subtype (Figs. 6e and 6f), suggesting significant heterogeneity in the epithelial component between the two samples.

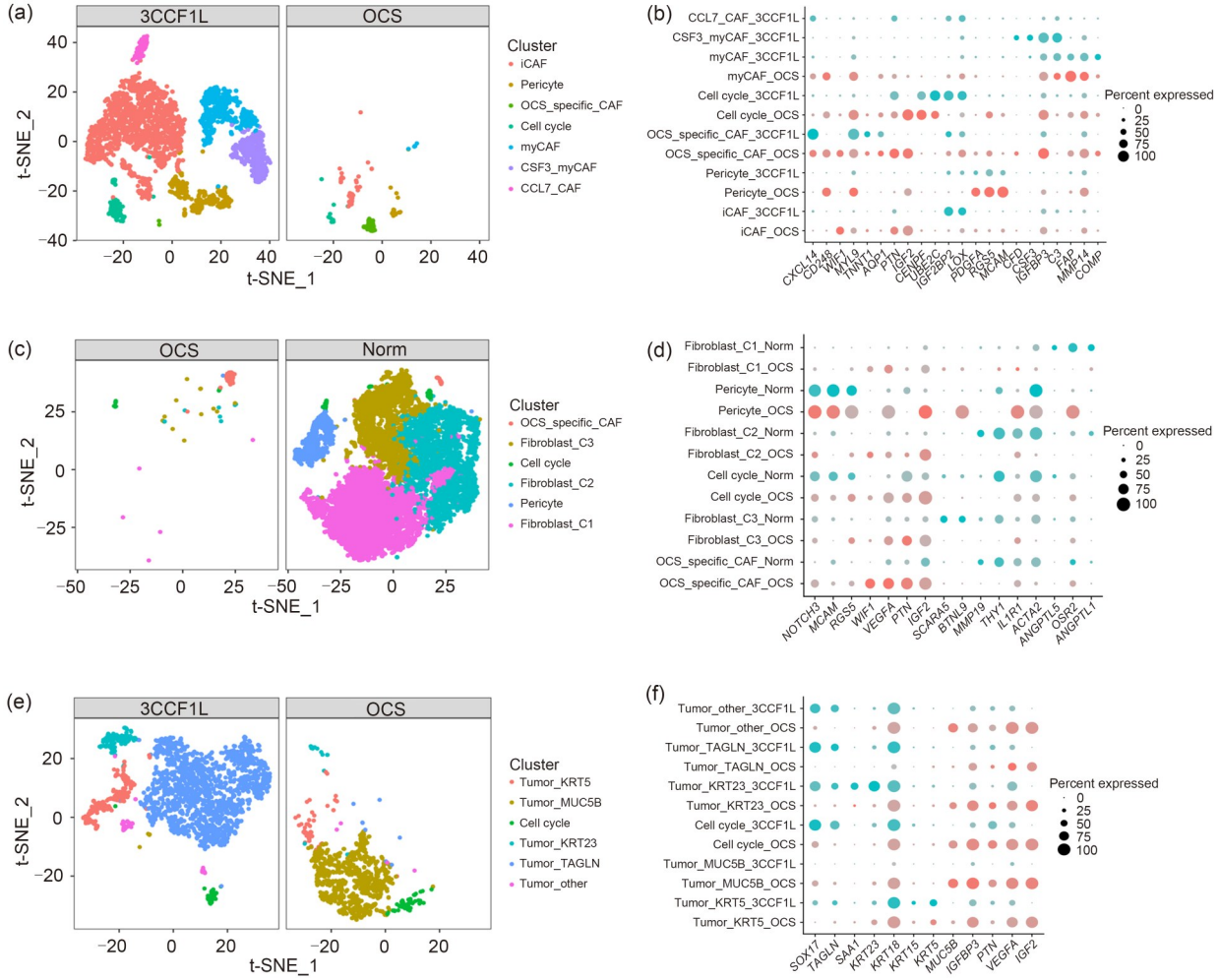


**Fig. 6 Comparison of single-cell RNA sequencing (scRNA-seq) data between ovarian carcinosarcoma (OCS) and the previously published OCS tumor and normal ovarian samples. (a, b) The t-distributed stochastic neighbor embedding (t-SNE) plots showing the distinct color-coded mesenchymal cell subclusters in this OCS tumor and the previously published OCS tumor (3CCF1L), and dot plot displaying the main marker genes in each mesenchymal cell subcluster. (c, d) t-SNE plots illustrating the distinct color-coded mesenchymal cell subclusters in this OCS tumor and the previously published normal (Norm) ovarian samples, and dot plot showing the main marker genes in each mesenchymal cell subcluster. (e, f) t-SNE plots presenting the different color-coded epithelial cell subclusters between the OCS tumor and the 3CCF1L tumor, and dot plot showing the main marker genes in each epithelial subcluster.**

## 3 Discussion

OCS shows a high degree of heterogeneity in terms of its aggressive tumor biology and is associated with poor survival outcomes. Given the rarity of OCS, it remains difficult to determine the best strategies for managing this malignancy. In the present work, we employed scRNA-seq to delineate a single-cell transcriptomic atlas of human OCS. The data obtained allowed us to identify unexpected biological features in distinct cell types, revealing novel cellular interactions between malignant epithelial and mesenchymal cells.

OCS is composed of both an epithelial component and a sarcomatous component (Boussios et al., 2019). The extent of contribution of each element in the development and progression of the malignancy differs; therefore, the preoperative diagnosis of this disease cannot be reliably made by fine-needle aspiration and core biopsy. In the present study, we analyzed 2173 cells of a single case of OCS, which led to the identification of nine cell types, including epithelial cells, fibroblasts, ovarian cortex cells, endothelial cells, T cells, NK cells, NKT cells, mast cells, and myeloid cells. Each subtype showed specific marker genes and pathway activities, suggesting that they represented distinct biological entities. Among all these cell types, epithelial cells accounted for the majority of cell populations in our scRNA-seq data, and these are considered to exert a pivotal role in OCS. The most frequently encountered epithelial elements were serous, endometrioid, and undifferentiated adenocarcinoma. However, the cellular diversity of epithelial cells, and how the epithelial subsets interact with OCS cells at the single-cell resolution, have not been well defined. Four distinct epithelial subtypes were found in OCS tissues, revealing the high intratumoral heterogeneity of OCS. Platinum and taxane-based chemotherapy is known to be the most common adjuvant treatment for OCS (del Carmen et al., 2012; Lamb et al., 2012; Kanis et al., 2016). However, OCS often recurs due to the development of chemoresistance and has poor survival outcomes. Moreover, the current second-line treatment options are limited. Therefore, it is urgent to clarify the potential molecular alterations to help our understanding of the tumor chemoresistance and ultimately to improve the treatment strategies for OCS. Advanced proteomic technologies, including mass spectrometry and protein array analysis, have significantly enhanced the exploration of the molecular signaling mechanisms in ovarian cancer. These approaches hold the potential to mitigate the development of drug resistance, leading to potentially enhanced patient outcomes (Ghose et al., 2022). In addition to proteomics, scRNA-seq also plays a role in revealing the mechanisms of tumor chemoresistance in ovarian cancer (Ghose et al., 2022). In the present study, we found that the epithelial cell subcluster 4 expressed high levels of two transcription factors BRCA1 and TOP2A and was enriched with drug-resistance genes. Of note, this epithelial subcluster also featured activated drug metabolic pathways, suggesting a potential association between the metabolism and drug resistance of tumor cells in OCS. Alterations in cellular metabolism have been previously shown to mediate the resistance of tumor cells to antitumor drugs (Chen et al., 2020). Intervening in the activity of these cell subclusters may help to restore cell sensitivity to chemotherapy. Furthermore, another published OCS sample was compared with our data of this OCS case, showing that the Tumor_MUC5B epithelial subtype was predominant in our OCS patient, whereas the Tumor_TAGLN epithelial subtype was primary from previously published OCS case (Regner et al., 2021). This difference indicates the significant heterogeneity of epithelial components between the two samples.

Besides the malignant epithelial cells, CNV analysis showed that the fibroblasts also displayed large chromosomal changes across the genome. The results of the present study suggested that mesenchymal cells were the main source of the malignant sarcomatous component of this OCS patient. We also demonstrated the presence of two mesenchymal cell subtypes. The C0 mesenchymal cells were the most prevalent mesenchymal cell subpopulation, expressing high levels of ECM signature genes. As the major component of the ECM, the collagen molecules including *COL6A2*, *COL6A1*, *COL3A1*, *COL6A3*, *COL5A2*, and *COL23A1* were enriched in this cluster. Pancreas cancer cells were reported to present increased proliferation and migration in the presence of type III collagen (Menke et al., 2001). In addition, collagen VI has direct stimulatory effects on cancer cells and also affects the TME via promoting inflammation and angiogenesis (Chen et al., 2013; Cescon et al., 2015). Of note, C0 mesenchymal cells also expressed genes related to

interferon-response genes, growth factors, as well as chemokines and interleukins, indicating the ability of this fibroblast subset to potentially modulate other cell component responses.

In order to determine the similarities and differences between OCS and HGSOC, we compared the malignant epithelial cells and mesenchymal cells of the OCS tumor with our published HGSOC scRNA-seq data (Xu et al., 2022). We found a similarity of epithelial cells of the OCS tumor to our HGSOC epithelial cells, especially in the HGSOC6 tumor. The mesenchymal cell subcluster C14 was specifically expressed in the OCS tumor with high levels of *CYP24A1*, *COL23A1*, *CCK*, *BMP7*, *PTN*, *WIF1*, and *IGF2*. Among them, it has been reported that *BMP7* expressed in the CAFs of prostate adenocarcinomas could stimulate the secretion of stromal cell-derived factor-1 (SDF-1) and induce angiogenic formation (Yang et al., 2008). IGF2 was found to be highly expressed in the CAFs of metastatic breast cancer and could promote tumor growth and suppress T-cell proliferation (Gui et al., 2019). Furthermore, we conducted a comparative analysis between our OCS tumor scRNA-seq data and a previously published OCS tumor dataset (Regner et al., 2021). Within our data, we identified that the mesenchymal cell subcluster C14, referred to as OCS_specific_CAFs, expressing *TNNT1* and *MYL9*, was associated with both rhabdomyosarcoma and sarcoma. This finding suggests the presence of rhabdomyosarcoma features in this cell subpopulation. Besides, in comparison to our previously published normal ovarian scRNA-seq data, we highlighted the heightened specificity of the OCS_specific_CAF subcluster within our OCS dataset compared to normal ovaries. These findings suggest that the mesenchymal cell subcluster C14 may play a significant role in the OCS tumor.

## 4 Conclusions

Taken together, we have revealed the transcriptome landscape in a primary OCS tumor at the single-cell resolution, which presents a well-established resource for elucidating OCS diversity. The findings of the present study may be used to advance the development and identification of therapeutic targets of this aggressive disease.

## Materials and methods

Detailed methods are provided in the electronic supplementary materials of this paper.

## Data availability statement

The scRNA-seq data of OCS have been deposited in Gene Expression Omnibus (GEO) with the accession number GSE185014.

## Acknowledgments

The research was supported by the National Natural Science Foundation of China (No. 82072855) and the Fundamental Research Funds for the Central Universities of China (No. 2023QZJH54).

## Author contributions

Junfen XU conceived and designed the study, performed experiments, analyzed the scRNA-seq data, and wrote and revised the manuscript. Mengyan TU performed the IHC experiments. Both authors have reviewed the manuscript and consented for publication, and therefore, have full access to all the data in the study and take responsibility for the integrity and security of the data.

## Compliance with ethics guidelines

Junfen XU is a Young Scientist Committee Member for *Journal of Zhejiang University-SCIENCE B (Biomedicine & Biotechnology)* and was not involved in the editorial review or the decision to publish this article. Junfen XU and Mengyan TU declare no conflicts of interest that pertain to this work.

This study was approved by the Ethics Committee of the Women's Hospital of Zhejiang University School of Medicine (No. IRB-20200346-R). Informed consent was acquired from the enrolled patient. All procedures followed were in accordance with the ethical standards of the responsible committee on human experimentation (institutional and national) and with the Helsinki Declaration of 1975, as revised in 2013.

## References

Ariyoshi K, Kawauchi S, Kaku T, et al., 2000. Prognostic factors in ovarian carcinosarcoma: a clinicopathological and immunohistochemical analysis of 23 cases. *Histopathology*, 37(5):427-436. https://doi.org/10.1046/j.1365-2559.2000.01015.x

Boussios S, Karathanasi A, Zakynthinakis-Kyriakou N, et al., 2019. Ovarian carcinosarcoma: current developments and future perspectives. *Crit Rev Oncol/Hematol*, 134:46-55. https://doi.org/10.1016/j.critrevonc.2018.12.006

Cescon M, Gattazzo F, Chen PW, et al., 2015. Collagen VI at a glance. *J Cell Sci*, 128(19):3525-3531. https://doi.org/10.1242/jcs.169748

Chen PW, Cescon M, Bonaldo P, 2013. Collagen VI in cancer and its biological mechanisms. *Trends Mol Med*, 19(7): 410-417.

https://doi.org/10.1016/j.molmed.2013.04.001

Chen X, Chen SW, Yu DS, 2020. Metabolic reprogramming of chemoresistant cancer cells and the potential significance of metabolic regulation in the reversal of cancer chemoresistance. *Metabolites*, 10(7):289. https://doi.org/10.3390/metabo10070289

Cheung A, Shah S, Parker J, et al., 2022. Non-epithelial ovarian cancers: how much do we really know? *Int J Environ Res Public Health*, 19(3):1106. https://doi.org/10.3390/ijerph19031106

del Carmen MG, Birrer M, Schorge JO, 2012. Carcinosarcoma of the ovary: a review of the literature. *Gynecol Oncol*, 125(1):271-277. https://doi.org/10.1016/j.ygyno.2011.12.418

Ding SN, Chen XS, Shen KW, 2020. Single-cell RNA sequencing in breast cancer: understanding tumor heterogeneity and paving roads to individualized therapy. *Cancer Commun*, 40(8):329-344. https://doi.org/10.1002/cac2.12078

Gao CX, Shi JM, Zhang JX, et al., 2022. Chemerin promotes proliferation and migration of ovarian cancer cells by upregulating expression of PD-L1. *J Zhejiang Univ-Sci B (Biomed & Biotechnol)*, 23(2):164-170. https://doi.org/10.1631/jzus.B2100392

Geistlinger L, Oh S, Ramos M, et al., 2020. Multiomic analysis of subtype evolution and heterogeneity in high-grade serous ovarian carcinoma. *Cancer Res*, 80(20):4335-4345. https://doi.org/10.1158/0008-5472.CAN-20-0521

George EM, Herzog TJ, Neugut AI, et al., 2013. Carcinosarcoma of the ovary: natural history, patterns of treatment, and outcome. *Gynecol Oncol*, 131(1):42-45. https://doi.org/10.1016/j.ygyno.2013.06.034

Ghose A, Gullapalli SVN, Chohan N, et al., 2022. Applications of proteomics in ovarian cancer: dawn of a new era. *Proteomes*, 10(2):16. https://doi.org/10.3390/proteomes10020016

Gotoh O, Sugiyama Y, Takazawa Y, et al., 2019. Clinically relevant molecular subtypes and genomic alteration-independent differentiation in gynecologic carcinosarcoma. *Nat Commun*, 10:4965. https://doi.org/10.1038/s41467-019-12985-x

Gui YR, Aguilar-Mahecha A, Krzemien U, et al., 2019. Metastatic breast carcinoma-associated fibroblasts have enhanced protumorigenic properties related to increased IGF2 expression. *Clin Cancer Res*, 25(23):7229-7242. https://doi.org/10.1158/1078-0432.CCR-19-1268

Hollis RL, Croy I, Churchman M, et al., 2022. Ovarian carcinosarcoma is a distinct form of ovarian cancer with poorer survival compared to tubo-ovarian high-grade serous carcinoma. *Br J Cancer*, 127(6):1034-1042. https://doi.org/10.1038/s41416-022-01874-8

Kanis MJ, Kolev V, Getrajdman J, et al., 2016. Carcinosarcoma of the ovary: a single institution experience and review of the literature. *Eur J Gynaecol Oncol*, 37(1):75-79.

Kurman RJ, Shih IM, 2011. Molecular pathogenesis and extraovarian origin of epithelial ovarian cancer—shifting the paradigm. *Hum Pathol*, 42(7):918-931. https://doi.org/10.1016/j.humpath.2011.03.003

Lamb MR, Gertsen E, Middlemas E, 2012. Carcinosarcoma of the ovary: case report and literature review. *Tenn Med*, 105(3):41-42.

Lee HW, Chung W, Lee HO, et al., 2020. Single-cell RNA sequencing reveals the tumor microenvironment and facilitates strategic choices to circumvent treatment failure in a chemorefractory bladder cancer patient. *Genome Med*, 12:47. https://doi.org/10.1186/s13073-020-00741-6

Liang LL, Yu J, Li J, et al., 2021. Integration of scRNA-seq and bulk RNA-seq to analyse the heterogeneity of ovarian cancer immune cells and establish a molecular risk model. *Front Oncol*, 11:711020. https://doi.org/10.3389/fonc.2021.711020

Liu C, Zhang Y, Li XH, et al., 2022. Ovarian cancer-specific dysregulated genes with prognostic significance: scRNA-seq with bulk RNA-seq data and experimental validation. *Ann N Y Acad Sci*, 1512(1):154-173. https://doi.org/10.1111/nyas.14748

Liu FS, Kohler MF, Marks JR, et al., 1994. Mutation and overexpression of the p53 tumor suppressor gene frequently occurs in uterine and ovarian sarcomas. *Obstet Gynecol*, 83(1):118-124.

Luo QK, Fu Q, Zhang X, et al., 2020. Application of single-cell RNA sequencing in pancreatic cancer and the endocrine pancreas. *In*: Yu BW, Zhang JQ, Zeng YM, et al. (Eds.), Single-cell Sequencing and Methylation. Springer, Singapore, p.143-152. https://doi.org/10.1007/978-981-15-4494-1_12

Ma XS, Guo JN, Liu KS, et al., 2020. Identification of a distinct luminal subgroup diagnosing and stratifying early stage prostate cancer by tissue-based single-cell RNA sequencing. *Mol Cancer*, 19:147. https://doi.org/10.1186/s12943-020-01264-9

Maynard A, McCoach CE, Rotow JK, et al., 2020. Therapy-induced evolution of human lung cancer revealed by single-cell RNA sequencing. *Cell*, 182(5):1232-1251.e22. https://doi.org/10.1016/j.cell.2020.07.017

Menke A, Philippi C, Vogelmann R, et al., 2001. Down-regulation of E-cadherin gene expression by collagen type I and type III in pancreatic cancer cell lines. *Cancer Res*, 61(8):3508-3517.

Näyhä V, Stenbäck F, 2008. Angiogenesis and expression of angiogenic agents in uterine and ovarian carcinosarcomas. *APMIS*, 116(2):107-117. https://doi.org/10.1111/j.1600-0463.2008.00757.x

Rauh-Hain JA, Growdon WB, Rodriguez N, et al., 2011. Carcinosarcoma of the ovary: a case-control study. *Gynecol Oncol*, 121(3):477-481. https://doi.org/10.1016/j.ygyno.2011.02.023

Rauh-Hain JA, Diver EJ, Clemmer JT, et al., 2013. Carcinosarcoma of the ovary compared to papillary serous ovarian carcinoma: a SEER analysis. *Gynecol Oncol*, 131(1):46-51. https://doi.org/10.1016/j.ygyno.2013.07.097

Regner MJ, Wisniewska K, Garcia-Recio S, et al., 2021. A multi-omic single-cell landscape of human gynecologic malignancies. *Mol Cell*, 81(23):4924-4941.e10.

https://doi.org/10.1016/j.molcel.2021.10.013

Siegel RL, Miller KD, Jemal A, 2020. Cancer statistics, 2020. *CA Cancer J Clin*, 70(1):7-30. https://doi.org/10.3322/caac.21590

Thompson SL, Compton DA, 2011. Chromosomes and cancer cells. *Chromosome Res*, 19(3):433-444. https://doi.org/10.1007/s10577-010-9179-y

Tong DL, Boocock DJ, Dhondalay GKR, et al., 2014. Artificial neural network inference (ANNI): a study on gene-gene interaction for biomarkers in childhood sarcomas. *PLoS ONE*, 9(7):e102483. https://doi.org/10.1371/journal.pone.0102483

Xu JF, Fang YF, Chen KL, et al., 2022. Single-cell RNA sequencing reveals the tissue architecture in human high-grade serous ovarian cancer. *Clin Cancer Res*, 28(16): 3590-3602. https://doi.org/10.1158/1078-0432.CCR-22-0296

Yang SX, Pham LK, Liao CP, et al., 2008. A novel bone morphogenetic protein signaling in heterotypic cell interactions in prostate cancer. *Cancer Res*, 68(1):198-205. https://doi.org/10.1158/0008-5472.CAN-07-5074

Zhao S, Xiong W, Xu K, 2020. MiR-663a, regulated by lncRNA GAS5, contributes to osteosarcoma development through targeting MYL9. *Hum Exp Toxicol*, 39(12):1607-1618. https://doi.org/10.1177/0960327120937330

Zhu J, Wen H, Ju XZ, et al., 2017. Clinical significance of programmed death ligand-1 and intra-tumoral $CD8^+$ T lymphocytes in ovarian carcinosarcoma. *PLoS ONE*, 12(1): e0170879. https://doi.org/10.1371/journal.pone.0170879

Zibetti Dal Molin G, Abrahão CM, Coleman RL, et al., 2018. Response to pembrolizumab in a heavily treated patient with metastatic ovarian carcinosarcoma. *Gynecol Oncol Res Pract*, 5:6. https://doi.org/10.1186/s40661-018-0063-3

Zorzou MP, Markaki S, Rodolakis A, et al., 2005. Clinicopathological features of ovarian carcinosarcomas: a single institution experience. *Gynecol Oncol*, 96(1):136-142. https://doi.org/10.1016/j.ygyno.2004.09.051

**Supplementary information**

Figs. S1–S4; Materials and methods